Photochemical & Photobiological Sciences

PAPER

View Article Online
View Journal | View Issue

Cite this: *Photochem. Photobiol. Sci.*, 2019, **18**, 1373

Diphenylaminostyryl-substituted quinolizinium derivatives as fluorescent light-up probes for duplex and quadruplex DNA†

Avijit Kumar Das, Heiko Ihmels * and Sarah Kölsch

Received 26th February 2019,
Accepted 10th March 2019

DOI: 10.1039/c9pp00096h

rsc.li/pps

(*E*)-2-[1′-((Diphenylamino)styryl)quinolizinium (**3a**) and 2,2′-{(phenylimino)-bis[(*E*)-1″,1‴-styryl]}-bis[quinolizinium] (**3b**) were synthesized, and their interactions with duplex DNA and quadruplex DNA were investigated with a particular focus on their ability to operate as DNA-sensitive fluorescent probes. Due to the significantly different size and steric demand of these quinolizinium derivatives they exhibit different binding modes. Thus, **3a** intercalates into duplex DNA and binds through π stacking to quadruplex DNA, whereas **3b** favours groove binding to both DNA forms. The emission intensity of these compounds is very low in aqueous solution, but it increases drastically upon association with duplex DNA by a factor of 11 (**3a**) and >100 (**3b**) and with quadruplex DNA by a factor of >100 (**3a**) and 10 (**3b**), with emission bands between 600 and 750 nm.

Introduction

The detection of nucleic acids is an important tool in clinical, forensic, and biological studies and applications.[1] And among the different chemical or biological tools that may be used for DNA analysis,[2] emission spectroscopy is one of the most versatile and efficient methods.[3] As a result, numerous fluorescent probes have been reported that allow the staining as well as qualitative and quantitative detection of DNA in cell-free medium and in cells.[4] Specifically, these molecular probes that indicate the nucleic acid selectively with an increase in the emission intensity upon association with the biomacromolecule (light-up probes) are very useful fluorimetric markers.[5] Along with the regular duplex DNA there is also an increasing interest in the detection of non-canonical DNA forms, with G-quadruplex DNA (G4-DNA) being the most prominent one. As this DNA form is proposed to have essential biological relevance and function,[6] probes have been developed recently that enable its selective fluorimetric detection.[7]

In this context, it has been demonstrated that styryl dyes with a cationic hetarene unit exhibit favourable properties for DNA sensing:[10–12] (i) the cationic charge of the dyes increases the affinity of the probe to DNA;[8] (ii) in donor–acceptor substituted styryl dyes ICT (intramolecular charge transfer) or TICT (twisted intramolecular charge transfer) states are possible, and these properties may change upon binding of the dye to DNA, thus enabling sensitive detection; and (iii) the large Stokes shifts in donor–acceptor substituted styryl dyes reduce the interference between excitation and detection light.[8,9] As a result, styryl dyes are widely used as probes in fluorescence-based bioanalytical applications, specifically DNA staining.[10–12]

In our studies on the development of DNA-sensitive fluorescent probes, we have demonstrated that annelated quinolizinium derivatives are versatile DNA-binding ligands that may be used for fluorimetric detection.[13] In addition, we have shown that especially donor-substituted quinolizinium derivatives have favourable photophysical properties and may therefore be used as versatile building blocks in fluorescent light-up probes.[14] Based on these observations we proposed that styryl-substituted quinolizinium derivatives may also be promising DNA-sensitive light-up probes with useful absorption and emission properties. So far, only a few styrylquinolizinium derivatives are known, and some of these have been already applied for fluorimetric DNA detection.[15] Among the derivatives investigated so far, the aminostyryl-substituted quinolizinium derivatives appeared to be the most promising candidates as they exhibit the typical advantages of donor–acceptor dyes. Therefore, we decided to vary this motif and employ a diphenylaminostyryl substituent as a donor unit, because the triarylamine unit is well known for its strong electron-donating properties,[16] and it was already shown to be a useful functionality in fluorescent chemosensors.[17] Herein, we present the synthesis of the resulting diphenylamino-substituted styrylquinolizinium derivatives **3a** and **3b** along with investigations of their interactions with duplex and quadruplex DNA with a

Department of Chemistry and Biology, University of Siegen, Center of Micro- and Nanochemistry and Engineering, Adolf-Reichwein-Str. 2, 57068 Siegen, Germany. E-mail: ihmels@chemie.uni-siegen.de

†Electronic supplementary information (ESI) available: Experimental procedures, additional spectroscopic data, and ^{1}H and ^{13}C NMR spectra of **3a** and **3b**. See DOI: 10.1039/c9pp00096h

particular focus on their potential application as DNA-sensitive fluorescent probes.

Results

Synthesis

The styrylquinolizinium derivatives **3a** and **3b** were synthesized by a Knoevenagel-condensation[18] of 2-methylquinolizinium (**1**)[19] with the mono- and diformyl-substituted triphenylamine derivatives **2a** and **2b**[20] in 70% and 67% yield, respectively (Scheme 1). The chemical structures of the ligands were confirmed by 1D and 2D ^{1}H NMR and ^{13}C NMR spectroscopy, mass spectrometry and elemental analysis (*cf.* ESI†).

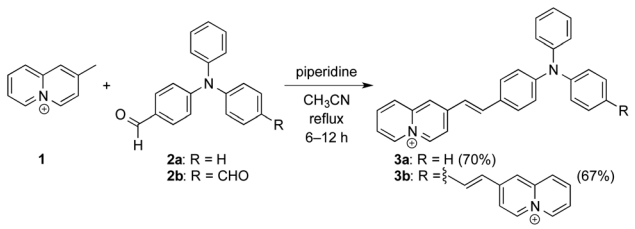

Scheme 1 Synthesis of styrylquinolizinium derivatives **3a** and **3b**.

Absorption and emission properties

The absorption and emission properties of compounds **3a** and **3b** were investigated in different solvents, namely CH_2Cl_2, $CHCl_3$, CH_3CN, MeOH, EtOH, DMSO and aqueous buffer at pH 7. The absorption spectra of **3a** and **3b** display a long-wavelength absorption maximum ranging from 450 nm (**3a**) and 473 nm (**3b**) in aqueous buffer to 500 nm (**3a**) and 512 nm (**3b**) in CH_2Cl_2 (Table 1, Fig. S1†). In most solvents, the emission intensity of derivatives **3a** and **3b** is very weak. Thus, in DMSO, MeOH, CH_3CN and buffer solution only a weak, broad emission band was observed between 600 and 750 nm, whereas in the protic polar solvent EtOH the emission intensity at 695 nm is slightly higher.

In contrast, both **3a** and **3b** show more intense emission in the less polar, chlorinated solvents $CHCl_3$ (**3a**: 638 nm, **3b**: 620 nm) and CH_2Cl_2 (**3a**: 695 nm, **3b**: 690 nm). In general, the emission quantum yields in $CHCl_3$ (Φ_{fl} = 0.34 and 0.27) are higher as compared to those in CH_2Cl_2 (Φ_{fl} = 0.21 and 0.12) (*cf.* ESI, Fig. S1, B1 and B2†).

To assess whether the low emission quantum yields of compounds **3a** and **3b** are caused by conformational changes in the excited state, the fluorescence spectra were recorded in media of high viscosity, namely aqueous solutions with increasing glycerol content.[22] Whereas in aqueous solution compounds **3a** and **3b** are basically non-fluorescent ($\Phi_{fl} \approx$ 0.002), an increasing content of glycerol (wt% glycerol: 0, 50, 100%) resulted in a large increase in the fluorescence quantum yield (Φ_{fl} = 0.30 for **3a** and Φ_{fl} = 0.14 for **3b**), along with a red shift of the absorption maxima from λ_{abs} = 450 nm to 472 nm (**3a**) and λ_{abs} = 473 nm to 493 nm (**3b**) (Fig. S2†).

Table 1 Absorption and emission properties of **3a** and **3b** in different solvents

Solvent	λ_{abs}[a]/nm	lg ε[b]	λ_{fl}[c]/nm	$\lambda_{abs} - \lambda_{fl}$[d]/cm^{-1}	Φ_{fl}[e]
3a					
$CHCl_3$	495	4.57	638	6993	0.34
CH_2Cl_2	500	4.56	695	5128	0.21
DMSO	458	4.55	725	3745	0.02
CH_3CN	460	4.58	736	3623	0.01
EtOH	472	4.59	695	4484	0.04
MeOH	465	4.60	710	4081	0.01
Buffer[f]	450	4.12	660	4716	<0.01
3b					
$CHCl_3$	513	4.71	620	9345	0.27
CH_2Cl_2	512	4.65	690	5617	0.12
DMSO	480	4.75	740	3846	<0.01
CH_3CN	480	4.77	738	3875	<0.01
EtOH	490	4.69	695	4878	0.03
MeOH	484	4.79	715	4329	0.02
Buffer[f]	473	4.23	682	4784	<0.01

[a] Long-wavelength absorption maximum; c = 10 μM. [b] ε = Molar extinction coefficient in cm^{-1} M^{-1}. [c] Fluorescence emission maximum; **3a**: λ_{ex} = 460 nm, **3b**: λ_{ex} = 500 nm. [d] Difference between absorption maximum and emission maximum at lowest energy. [e] Fluorescence quantum yield relative to rhodamine B in EtOH (Φ_{fl} = 0.7) (ref. 21). [f] In 10 mM BPE buffer solution at pH 7.0 and 20 °C.

DNA binding properties

Spectrophotometric and spectrofluorimetric titrations. The interactions of derivatives **3a** and **3b** with calf thymus (ct) DNA and the quadruplex forming oligonucleotide d[A(GGGTAA)$_3$GGG] (**22AG**) were monitored by photometric and fluorimetric titrations in BPE buffer solution (ct DNA) or in K-phosphate buffer (**22AG**) at 20 °C and pH 7 (Fig. 1 and 2). In both cases, the absorption spectrum of the quinolizinium derivatives **3a**

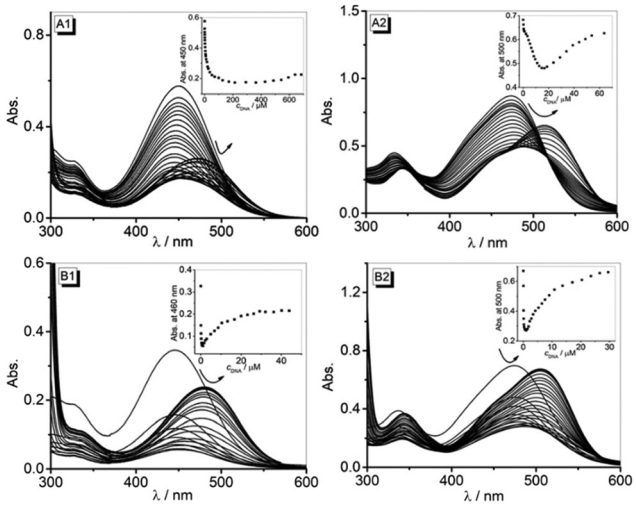

Fig. 1 Photometric titration of **3a** (1) and **3b** (2) with ct DNA (A, c = 1.88 mM in base pairs) in BPE buffer (10 mM, pH 7.0; solutions of ligands with 10% v/v DMSO, c_{Ligand} = 20 μM) and with **22AG** (B, c = 200 μM) in K-phosphate buffer at pH 7.0 at 20 °C (c_{Ligand} = 20 μM). The arrows indicate the changes of absorption upon addition of DNA. Inset: Changes of the ligand absorption with increasing DNA concentration.

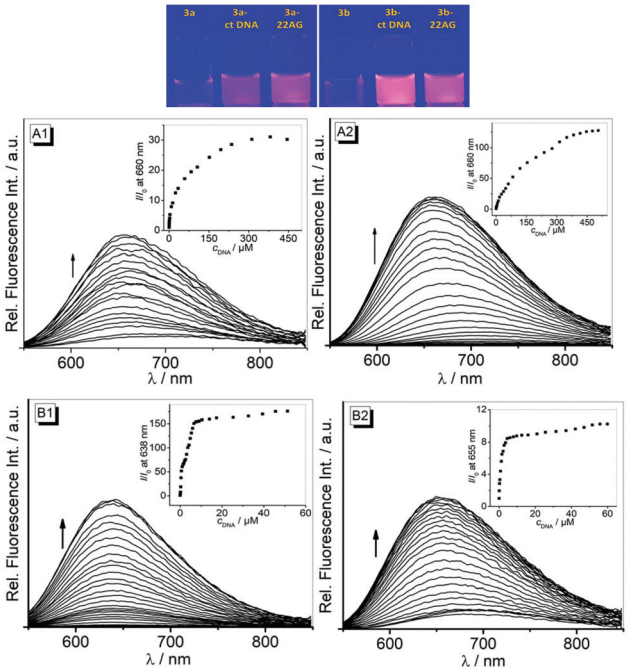

Fig. 2 Fluorimetric titration of **3a** (1) and **3b** (2) (c = 10 μM) with ct DNA (A, c = 1.88 mM) in BPE buffer (10 mM; solutions of ligands with 10% v/v DMSO) and with **22AG** (B, c = 200 μM) in K-phosphate buffer; pH = 7.0, T = 20 °C, **3a**: λ_{ex} = 460 nm, **3b**: λ_{ex} = 500 nm. The arrows indicate the changes of emission intensity upon addition of DNA. Inset: Plot of relative fluorescence intensity of **3a** and **3b** *versus* c_{DNA} (corrected with regard to the change of the absorption at the excitation wavelength). Top: Pictures of emission color of **3a** and **3b** in the absence and presence of DNA.

and **3b** changed significantly upon addition of ct DNA and **22AG**. Thus, upon addition of ct DNA to a solution of **3a** or **3b**, the absorbance of these compounds firstly decreased with a slight red shift on addition of ct DNA until ligand–DNA ratios (LDR) of >1.4 (**3a**) and >0.2 (**3b**) were achieved. Further addition of ct DNA led to an increase in the absorbance with a red shift of the absorption maximum to 470 nm ($\Delta\lambda$ = 20 nm; **3a**) and 513 nm ($\Delta\lambda$ = 40 nm, **3b**) (Fig. 1A). On titration of **22AG** to compounds **3a** and **3b** the absorbance at 450 nm (**3a**) and 473 nm (**3b**) decreased until LDRs of >20 (**3a**) and >18.6 (**3b**) were achieved. At a higher concentration of **22AG** (LDR <0.4 and <0.7, resp.) a red shifted absorption peak was formed at 480 nm ($\Delta\lambda$ = 30 nm) (**3a**) and 505 nm ($\Delta\lambda$ = 32 nm) (**3b**) (Fig. 1B). The data from spectrophotometric titrations were used to determine the binding constant, K_b, obtained from the fitting of the experimental binding isotherms to the theoretical model (*cf.* ESI, Fig. S3†).[24] Thus, ligands **3a** and **3b** bind to ct DNA with binding constants of $K_b = 4.3 \times 10^4$ M^{-1} and $K_b = 8.8 \times 10^4$ M^{-1}.

The emission intensities of both compounds **3a** and **3b** increased significantly in the presence of DNA (Fig. 2). Thus, the addition of ct DNA and **22AG** to derivative **3a** resulted in a continuous increase of the weak emission band by a factor of 30 (ct DNA, Φ_{fl} = 0.16) and 176 (**22AG**, Φ_{fl} = 0.26) and small blue shifts ($\Delta\lambda \approx 20$ nm) of the emission maximum (Fig. 2, A1 and B1).

Similarly, the weak emission of compound **3b** increased by factors of 128 and 10 on addition of ct DNA (Φ_{fl} = 0.40) and **22AG** (Φ_{fl} = 0.13), respectively, and the emission maxima were slightly blue shifted to 660 nm and 655 nm on addition of ct DNA and **22AG** (Fig. 2, A2 and B2). From the fluorescence titration experiments, the limit of detection (LOD) of **3a** and **3b** was estimated to be 0.02 μM and 0.79 μM for ct DNA and 0.05 μM and 0.01 μM for **22AG**, respectively (*cf.* ESI, Table S1†).[23]

To check whether the fluorimetric analysis is disturbed by the formation of singlet oxygen and subsequent DNA damage, the irradiation of a **3b**–DNA complex (LDR = 0.3) under aerobic conditions was monitored by CD spectroscopy (*cf.* ESI, Fig. S5†). Under these conditions, no significant changes in the CD signals corresponding to the DNA absorption (<300 nm) were observed, which indicates negligible changes in the DNA structure after irradiation. In another experiment, we examined the influence of oxygen on the excited singlet state of **3b** by recording emission spectra at different oxygen concentrations. Namely, the spectra were measured under anaerobic conditions, in air or in oxygen-saturated solution under otherwise identical conditions (*cf.* ESI, Fig. S6†). Notably, the fluorescence intensity of ligand **3b** and of the **3b**–ct DNA complex is essentially independent of the oxygen concentration, which indicates that oxygen does not significantly quench the excited singlet state.

CD- and LD-spectroscopic analysis

Complementary analysis with circular dichroism (CD) and *flow* linear dichroism (LD) spectroscopy revealed that in the presence of ct DNA, ligands **3a** and **3b** display induced circular dichroism (ICD) and LD bands in the absorption range of the ligands (Fig. 3). A solution of ligand **3a** with ct DNA exhibited negative ICD bands at 247 nm, 310 nm, 420 nm and 500 nm, all of which increased in intensity from LDR = 0.3 to 1.0. At higher LDR values, however, the negative long-wavelength bands at 420 nm and 500 nm developed into a very intense bisignate band with zero transition at the absorption maximum. Simultaneously, the initially intense positive CD signal of the DNA at 278 nm decreased drastically (Fig. 3, A1). At the same time, the addition of ct DNA to the solution of ligand **3a** (LDR = 0–1.0) led to the formation of a gradually increasing negative LD signal in the absorption region of the ligand (350–550 nm). Notably, the intensity of the negative LD signal at 258 nm decreased with increasing LDR values (Fig. 3, B1).

The complexation of compound **3b** with ct DNA resulted in the formation of positive ICD signals at 347 nm and 545 nm, along with a negative signal at 460 nm. Up to an LDR value of 0.5, the intensities of the two very strong positive CD bands at 545 nm and 460 nm increased, but at a larger LDR of 1.0 these CD bands decreased (Fig. 3, A2). The LD spectra of complexes of **3b** and ct DNA revealed a very strong positive band at 536 nm that increased from LDR = 0.3 to 0.5 and subsequently disappeared at larger LDR = 1 in favour of a weak bisignate band with maxima at 540 nm and 440 nm. Concurrently, very

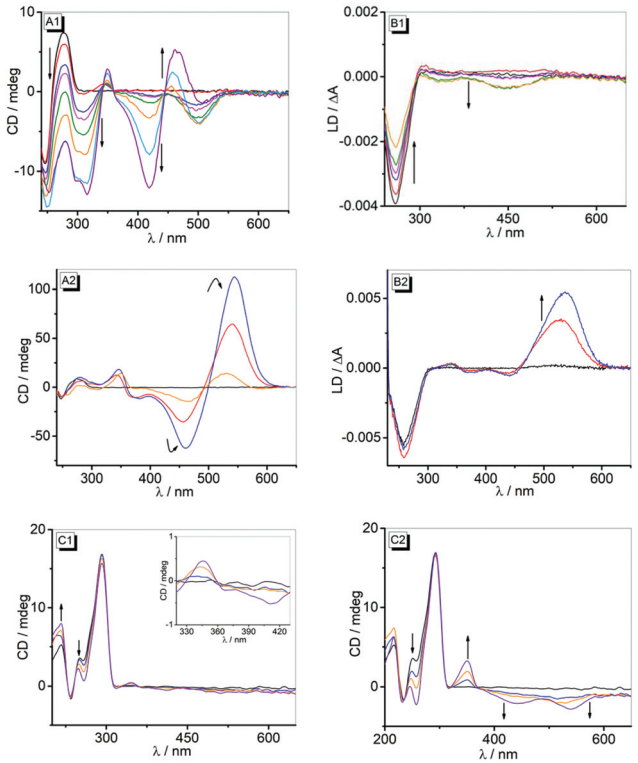

Fig. 3 CD spectra (A) and LD spectra (B) of ct DNA (c = 50 μM) in the absence and presence of **3a** (1) and **3b** (2) at LDR = 0 (black), 0.3 (red), 0.5 (blue), 0.6 (magenta), 0.8 (green), 1.0 (orange), 1.5 (cyan), 2.0 (violet) in BPE buffer solution (10 mM, pH 7.0; solutions of ligands with 10% v/v DMSO). CD spectra of **22AG** (c = 20 μM) in the absence and presence of **3a** (C1) and **3b** (C2) at LDR = 0 (black), 0.5 (blue), 1.0 (orange), 2.0 (violet) in K-phosphate buffer at pH 7 at 20 °C (solutions of ligands with 1% DMSO).

weak positive and negative LD signals were observed at 340 nm (+), 375 nm (−) and 440 nm (−) that strongly broadened with increasing LDR values (Fig. 3, B2).

On addition of derivatives **3a** and **3b** to G4-DNA **22AG** the characteristic CD pattern of the hybrid-type structure of the quadruplex, *i.e.* with positive bands at 290 nm and 270 nm along with a negative band at 235,[25] did not change essentially (Fig. 3, C1 and C2). In the complex of **3a** and **22AG**, only a very weak bisignate ICD band was observed with maxima at 345 nm (+) and 410 nm (−) (Fig. 3, C1). In contrast, more pronounced ICD signals developed in the absorption range of the derivative **3b** upon addition of G4-DNA **22AG**. Specifically, with increasing LDR from 0 to 2.0, a positive band at 350 nm and two very broad negative bands with maxima at 440 nm and 540 nm were observed (Fig. 3, C2). CD-spectroscopic analysis was also performed to determine the influence of the association of **3a** and **3b** on the quadruplex melting temperature, T_m (*cf.* ESI, Fig. S7†). Thus, the determination of the DNA melting temperature by monitoring the temperature-dependent CD intensity revealed an increase in the melting temperature, ΔT_m, in the presence of the ligands (**3a:** ΔT_m = 3 °C, **3b:** ΔT_m = 9 °C, at LDR = 2).

Discussion

The absorption and emission properties of **3a** and **3b** in different solvents resemble the ones that have been reported previously for styryl substituted quinolizinium derivatives.[15d] Although the absorption and emission shifts of these compounds are slightly different in various polar aprotic and polar protic solvents (Table 1), there was no clear relationship identified between the absorption and emission energy and a particular solvent property. This observation indicates that several solvent properties, such as polarity and hydrogen bonding, contribute to the overall solvent effect to different extents. Notably, in CH_2Cl_2 and $CHCl_3$, derivatives **3a** and **3b** exhibit significant red shifts of the absorption bands (Fig. S1†) which are frequently observed for cationic dyes due to the high polarizability of chloroalkane solvents.[26] In addition, it should be considered that these compounds are poorly soluble in these solvents, which leads to dye aggregation. Thus, the red-shifted absorption in these solvents may indicate the aggregate formation.[27] The emission intensity of **3a** and **3b** is very low in polar solvents (<0.04), most likely due to the radiationless deactivation of the excited state by conformational changes, such as rotation about the vinyl–arene bond, as commonly observed for styryl dyes.[28] This assumption was clearly supported by the observation that the emission intensity increases with increasing viscosity of the solution, namely in glycerol–water mixtures (*cf.* ESI, Fig. S2†), as the rotational relaxation of the excited molecule becomes slower than the fluorescence at higher viscosity. Presumably, the slightly larger emission quantum yields of **3a** and **3b** in $CHCl_3$ and CH_2Cl_2 (Φ_{fl} = 0.1 to 0.3) are the result of their low solubility in these solvents and are thus caused by an aggregation-induced enhancement of the emission intensity.[29]

The binding studies of **3a** and **3b** with ct DNA and **22AG** by photometric, fluorimetric and polarimetric titrations clearly confirmed the association of these ligands with DNA. Firstly, the photometric titrations show a development of absorption bands that is characteristic of DNA-binding ligands, *i.e.* a hypochromic effect along with a red shift of the absorption band with progressing titration of DNA.[30] Nevertheless, the lack of isosbestic points and the appearance of two distinctly different sections of the titration (Fig. 1) point to different binding modes that depend on the LDR. Thus, at the beginning of the titration, *i.e.* at large LDR values, the ligands form aggregates along the DNA backbone because there are not enough binding sites available. At smaller LDR values, *i.e.* with ample number of binding sites, the ligands may associate with the DNA by intercalation or groove binding. Notably, the sterically demanding diphenylamino-substituent severely hinders the access of a ligand close to an already occupied DNA binding site, which explains the large amount of DNA required to reach saturation. Unfortunately, this heterogeneous binding of both ligands with duplex and quadruplex DNA, that even changes in the course of the titrations, seriously hampers the determination of meaningful binding constants from the binding isotherms, as the ones calculated only reflect an apparent binding constant, *i.e.* an average constant from all

contributing binding modes, thus showing different overall affinities of the ligands toward a particular DNA form. Hence, the apparent binding constants of ligands **3a** and **3b** with ct DNA show a higher overall affinity of **3b** to this DNA form. The K_b values (**3a**: $K_b = 4.3 \times 10^4\ M^{-1}$, **3b**: $K_b = 8.8 \times 10^4\ M^{-1}$) differ only by a factor of *ca.* 2 and are both comparable to the ones obtained for classical intercalators.[30]

Additional information about the binding mode was obtained by CD- and LD-spectroscopic studies. Thus, the strong bisignate ICD band in the long-wavelength absorption range of compound **3a** at high LDR clearly confirms the aggregation of the dye at the DNA backbone (Fig. 3, A1).[31] At lower LDR, a less intense negative ICD band appears, which indicates a different binding mode. But it should be noted that the latter band is still overlapped by the ICD signal of the aggregate, resulting in a combination of spectra that cannot be dissected. Similarly, the CD bands in the absorption range of DNA and the ligand (<320 nm) also severely overlap. As a result, this combination of overlapping bands, whose contribution also changes with LDR, does not allow a conclusive binding mode analysis at low LDR. At the same time, the negative LD signal in the absorption range of **3a** (Fig. 3, B1) clearly indicates an intercalative binding mode of this ligand with ct DNA.[32]

In the case of ligand **3b**, the very intense bisignate CD signal between 400 nm and 600 nm is maintained at all employed LDR ratios, and in each case the bands correspond to the two absorption maxima observed during photometric titration (Fig. 3 A2 and B2). This observation shows that this CD spectrum is also a combination of separate bands. Notably, the ICD bands of the ligand are very strong, as seen directly from the comparison with the DNA bands, and this is usually observed for groove binders.[33] The LD-spectroscopic analysis supports this interpretation, as the positive LD band at the long-wavelength absorption of the ligand unambiguously indicates groove binding.[31] The weak positive LD bands at 375 nm and 440 nm seem to contradict the latter interpretation, but it should be noted that the size and shape of the ligand do not allow for a complete accommodation and fit of the whole molecule within the groove, so that at least partially one of the quinolizinium units point outside the groove or even intercalate. In this arrangement, this quinolizinium chromophore is decoupled from the conjugated π system and essentially oriented in the same direction as the DNA bases, thus resulting in a positive LD signal.[31] Such bisignate LD spectra have also been observed with bichromophoric bis-aminonaphthalimide-substituted Tröger bases and interpreted similarly.[34] It is worth noting, however, that the intensity of CD and LD signals decreased significantly at higher LDR, presumably because at this higher ligand loading there are not sufficient binding sites available in the grooves, thus reducing the relative number of intercalated or groove-bound ligands.

The two ligands **3a** and **3b** do not carry special substituents that may be involved in specific interactions with the DNA, such as hydrogen bonding. Even the amino group is not available as it is sterically protected and the free lone pair of the amino group is highly delocalized. Therefore, the association of these ligands should be mainly governed by attractive dispersion interactions, such as π stacking and van der Waals interactions, with the binding site and by the thermodynamically favorable counter-ion release from the DNA upon association of the cationic ligand.[35] Therefore, the different binding modes of ligands **3a** and **3b** are mainly based on their different size and shape. Both compounds are structurally flexible containing triphenylamine as a rather hydrophobic unit and the quinolizinium as the DNA-binding fragment. In the case of **3a**, the bulky diaryl unit may point outside the binding site or even accommodate partly in the groove when the quinolizinium intercalates into DNA. Obviously, this binding mode is not favoured with **3b** as only one of the two quinolizinium units can intercalate and the majority of the molecule would still protrude from the binding site so that it is still exposed to the solvent, thus reducing the role of the hydrophobic effect as a driving force for intercalation.[35] As a result, ligand **3b** binds to the grooves because in this binding mode this sterically demanding molecule fits better to the binding site as a whole, which may be driven by entropic factors.[36]

The association of **3a** and **3b** with G4-DNA **22AG** was confirmed with CD spectroscopy. In the presence of **3a** and **3b**, the CD bands of the quadruplex **22AG** change only marginally (Fig. 3, C1 and C3), which indicates the preservation of the quadruplex structure upon complex formation.[37] The complex formation is also clearly indicated by the increased melting temperature, ΔT_m, of the quadruplex in the presence of ligands **3a** and **3b**, which indicates significant thermodynamic stabilization of the quadruplex toward unfolding due to ligand association. At the same time, the disappearance of the weak shoulder around 250 nm usually denotes the disappearance of one minor form from the equilibrium of different quadruplex structures because of the stabilization of a basket-type or chair-type quadruplex structure by the ligand.[38] In the case of ligand **3a**, only a very weak ICD signal in the absorption range of the ligand developed, which is often observed for ligands that bind to the quadruplex by terminal π stacking.[39] In contrast, the association of ligand **3b** with **22AG** leads to the formation of a much more pronounced ICD signal, which is proposed to be a characteristic feature of groove-binding G4-DNA ligands.[40]

In the absence of DNA, the styrylquinolizinium derivatives **3a** and **3b** are weakly fluorescent with very low quantum yields in aqueous buffer solution (Table 1) due to radiationless deactivation by conformational relaxation of the excited state (see Discussion above). Upon association with duplex and quadruplex DNA, however, the emission intensity of these ligands increases significantly (Fig. 2). As observed for several DNA-sensitive fluorescent light-up probes,[14,15] this effect is most likely the result of the restricted conformational freedom of movement of the ligand within the binding site,[41] which is comparable to the light-up effect observed in glycerol.[22] Similar fluorescence light-up effects on DNA binding have been observed with annelated quinolizinium derivatives[42] and diphenylamino-substituted derivatives of quinolinium, pyridinium and imidazolium.[43]

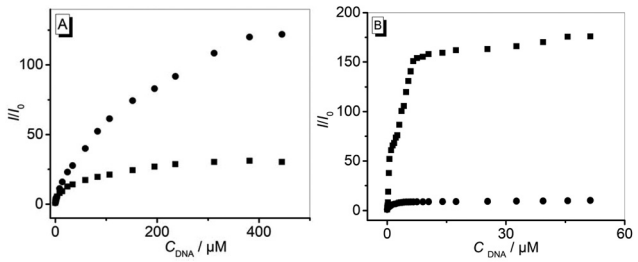

Fig. 4 Plot of relative emission intensity I/I_0 of **3a** (squares) and **3b** (circles) (c = 10 μM) *versus* concentration of ct DNA in BPE buffer (10 mM, pH 7.0; with 10% v/v DMSO) and **22AG** in K-phosphate buffer; pH 7.0, T = at 20 °C.

Most interesting is the observation that the fluorescence light-up effect of **3b** on binding with ct DNA is 4 times stronger than that of **3a** (Fig. 4A). Considering that the light-up effect is mainly caused by the restricted conformational flexibility of the ligand in the sterically constrained binding site, and not necessarily with the binding strength, this observation indicates that the groove-bound ligand **3b** is accommodated more tightly in its binding site than the intercalated molecule **3a**. Conversely, when bound to G4-DNA, the light-up factor of **3a** is 17 times larger than that of **3b** (Fig. 4B), so that in this case the conformational flexibility of **3a** is more suppressed in the DNA binding site.

Conclusion

In summary, it was demonstrated that the diphenylaminostyryl-substituted quinolizinium derivatives **3a** and **3b** bind to duplex and quadruplex DNA. Due to the significantly different size and steric demand of these ligands they exhibit different binding modes. Thus, **3a** intercalates into ct DNA and binds through π stacking to G4-DNA **22AG**, whereas **3b** favours groove binding to both DNA forms. As the very low emission intensity of these compounds increases strongly upon association with DNA and the emission wavelength is close to the NIR range, which is favourable for biological applications, these compounds are promising platforms for the development of DNA-sensitive fluorescent probes. In this regard, the different effects of the actual DNA form and binding mode on the extent of the light-up effect may be used for selective DNA detection.

Conflicts of interest

There are no conflicts to declare.

Acknowledgements

We thank the University of Siegen and the Alexander von Humboldt Foundation (postdoctoral research fellowship for A. K. D.) for financial support. We thank Ms Jennifer Hermann and Ms Sandra Uebach for technical assistance.

Notes and references

1 (*a*) P. B. Dervan, Molecular recognition of DNA by small molecules, *Bioorg. Med. Chem.*, 2001, **9**, 2215–2235; (*b*) J. Sheng, J. Gan and Z. Huang, Structure-based DNA-targeting strategies with small molecule ligands for drug discovery, *Med. Res. Rev.*, 2013, **33**, 1119–1173; (*c*) J. Wang, Survey and summary: From DNA biosensors to gene chips, *Nucleic Acids Res.*, 2000, **28**, 3011–3016; (*d*) L. H. Hurley, DNA and its associated processes as targets for cancer therapy, *Nat. Rev. Cancer*, 2002, **2**, 188–200; (*e*) P. G. Baraldi, A. Bovero, F. Fruttarolo, D. Preti, M. A. Tabrizi, M. G. Pavani and R. Romagnoli, DNA minor groove binders as potential antitumor and antimicrobial agents, *Med. Res. Rev.*, 2004, **24**, 475–528.

2 (*a*) N. C. Seeman and H. F. Sleiman, DNA nanotechnology, *Nat. Rev. Mater.*, 2017, **3**, 17068; (*b*) Y. Jung and S. J. Lippard, Direct Cellular Responses to Platinum-Induced DNA Damage, *Chem. Rev.*, 2007, **107**, 1387–1407; (*c*) J. Wu, Y. Zou, C. Li, W. Sicking, I. Piantanida, T. Yi and C. Schmuck, A Molecular Peptide Beacon for the Ratiometric Sensing of Nucleic Acids, *J. Am. Chem. Soc.*, 2012, **134**, 1958–1961; (*d*) H. Song, J. T. Kaiser and J. K. Barton, Crystal structure of Δ-$[Ru(bpy)_2dppz]^{2+}$ bound to mismatched DNA reveals side-by-side metalloinsertion and intercalation, *Nat. Chem.*, 2012, **4**, 615–620.

3 (*a*) H. Kobayashi, M. Ogawa, R. Alford, P. L. Choyke and Y. Urano, New Strategies for Fluorescent Probe Design in Medical Diagnostic Imaging, *Chem. Rev.*, 2010, **110**, 2620–2640; (*b*) D.-L. Ma, H.-Z. He, K.-H. Leung, H.-J. Zhong, D. S.-H. Chan and C.-H. Leung, Label-free luminescent oligonucleotide-based probes, *Chem. Soc. Rev.*, 2013, **42**, 3427–3440.

4 (*a*) Y. V. Suseela, N. Narayanaswamy, S. Pratihar and T. Govindaraju, Far-red fluorescent probes for canonical and non-canonical nucleic acid structures: current progress and future implications, *Chem. Soc. Rev.*, 2018, **47**, 1098–1131; (*b*) S. J. Smith, C. R. Nemr and S. O. Kelley, Chemistry-Driven Approaches for Ultrasensitive Nucleic Acid Detection, *J. Am. Chem. Soc.*, 2017, **139**, 1020–1028; (*c*) S. Manna and S. G. Srivatsan, Fluorescence-based tools to probe G-quadruplexes in cell-free and cellular environments, *RSC Adv.*, 2018, **8**, 25673–25694; (*d*) D. Wu, A. C. Sedgwick, T. Gunnlaugsson, E. U. Akkaya, J. Yoon and T. D. James, Fluorescent chemosensors: the past, present and future, *Chem. Soc. Rev.*, 2017, **46**, 7105–7123.

5 (*a*) P. Prentø, A contribution to the theory of biological staining based on the principles for structural organization of biological macromolecules, *Biotech. Histochem.*, 2001, **76**, 137–161; (*b*) J. B. LePecq and C. A. Paoletti, A fluorescent complex between ethidium bromide and nucleic acids. Physical-chemical characterization, *J. Mol. Biol.*,

1967, **27**, 87–106; (*c*) L. S. Lermann, Structural considerations in the interaction of DNA and acridines, *J. Mol. Biol.*, 1961, **3**, 18–30; (*d*) A. Slama-Schwok, J. Jazwinski, A. Bere, T. Montenay-Garestier, M. Rougée, C. Hélène and J. M. Lehn, Interactions of the Dimethyldiazaperopyrenium Dication with Nucleic Acids. 1. Binding to Nucleic Acid Components and to Single-Stranded Polynucleotides and Photocleavage of Single-Stranded Oligonucleotides, *Biochemistry*, 1989, **28**, 3227–3234.

6 (*a*) S. Neidle, Quadruplex nucleic acids as targets for anticancer therapeutics, *Nat. Rev. Chem.*, 2017, **1**, UNSP 0041; (*b*) D.-L. Ma, Z. Zhang, M. Wang, L. Lu, H. J. Zhong and C.-H. Leung, Recent Developments in G-Quadruplex Probes, *Chem. Biol.*, 2015, **22**, 812–828; (*c*) S. Neidle, Quadruplex Nucleic Acids as Novel Therapeutic Targets, *J. Med. Chem.*, 2016, **59**, 5987–6011.

7 (*a*) Y. Xu, Chemistry in human telomere biology: structure, function and targeting of telomere DNA/RNA, *Chem. Soc. Rev.*, 2011, **40**, 2719–2740; (*b*) A. Ali and S. Bhattacharya, DNA binders in clinical trials and chemotherapy, *Bioorg. Med. Chem.*, 2014, **22**, 4506–4521; (*c*) P. Murat, Y. Singh and E. Defrancq, Methods for investigating G-quadruplex DNA/ligand interactions, *Chem. Soc. Rev.*, 2011, **40**, 5293–5307; (*d*) E. Largy, A. Granzhan, F. Hamon, D. Verga and M. P. Teulade-Fichou, Visualizing the quadruplex: from fluorescent ligands to light-up probes, *Top. Curr. Chem.*, 2013, **330**, 111–177.

8 (*a*) R. W. Sinkeldam, N. J. Greco and Y. Tor, Fluorescent Analogs of Biomolecular Building Blocks: Design, Properties, and Applications, *Chem. Rev.*, 2010, **110**, 2579–2619; (*b*) T. Deligeorgiev, A. Vasilev, S. Kaloyanova and J. J. Vaquero, Styryl dyes – synthesis and applications during the last 15 years, *Color. Technol.*, 2010, **126**, 55–80; (*c*) G. R. Rosania, J. W. Lee, L. Ding, H. S. Yoon and Y. T. Chang, Combinatorial Approach to Organelle-Targeted Fluorescent Library Based on the Styryl Scaffold, *J. Am. Chem. Soc.*, 2003, **125**, 1130–1131.

9 (*a*) H. Özhalici-Ünal, C. L. Pow, S. A. Marks, L. D. Jesper, G. L. Silva, N. I. Shank, E. W. Jones, J. M. Burnette, P. B. Berget and B. A. Armitage, A Rainbow of Fluoromodules: A Promiscuous scFv Protein Binds to and Activates a Diverse Set of Fluorogenic Cyanine Dyes, *J. Am. Chem. Soc.*, 2008, **130**, 12620–12621; (*b*) A. Ajayaghosh, E. Arunkumar and J. Daub, A Highly Specific Ca^{2+}-Ion Sensor: Signaling by Exciton Interaction in a Rigid–Flexible–Rigid Bichromophoric "H" Foldamer, *Angew. Chem., Int. Ed.*, 2002, **41**, 1766–1769.

10 (*a*) R. W. Dirks and H. J. Tanke, Styryl Molecules Light-Up RNAs, *Chem. Biol.*, 2006, **13**, 559–561; (*b*) C. V. Kumar, R. S. Turner and E. H. Asuncion, Groove binding of a styryl cyanine dye to the DNA double helix: the salt effect, *J. Photochem. Photobiol., A*, 1993, **74**, 231–238; (*c*) N. Akbay, M. Y. Losytskyy, V. B. Kovalska, A. O. Balanda and S. M. Yarmoluk, The Mechanism of Benzothiazole Styryl cyanine Dyes Binding with dsDNA: Studies by Spectral-Luminescent Methods, *J. Fluoresc.*, 2008, **18**, 139–147; (*d*) N. Nizomov, E. N. Kurtaliev, S. N. Nizamov and G. Khodjayev, Spectral-luminescent study of the interaction of some styrylcyanine dyes with bovine serum albumin and DNA in aqueous solutions, *J. Mol. Struct.*, 2009, **936**, 199–205.

11 (*a*) V. B. Kovalska, D. V. Kryvorotenko, A. O. Balanda, M. Y. Losytskyy, V. P. Tokar and S. M. Yarmoluk, Fluorescent homodimer styrylcyanines: synthesis and spectral-luminescent studies in nucleic acids and protein complexes, *Dyes Pigm.*, 2005, **67**, 47–54; (*b*) J.-S. Lee, Y. K. Kim, M. Vendrel and Y.-T. Chang, Diversity-oriented fluorescence library approach for the discovery of sensors and probes, *Mol. BioSyst.*, 2009, **5**, 411–421; (*c*) D. V. Berdnikova, O. A. Fedorova, E. V. Tulyakova, H. Li, S. Kölsch and H. Ihmels, Interaction of Crown Ether-Annelated Styryl Dyes with Double-Stranded DNA, *Photochem. Photobiol.*, 2015, **91**, 723–731; (*d*) A. Mazzoli, B. Carlotti, G. Consiglio, C. G. Fortuna, G. Miolo and A. Spalletti, Photobehaviour of methyl-pyridinium and quinolinium iodide derivatives, free and complexed with DNA. A case of bisintercalation, *Photochem. Photobiol. Sci.*, 2014, **13**, 939–950; (*e*) M.-Q. Wang, J. Xu, L. Zhang, Y. Liao, H. Wei, Y.-Y. Yin, Q. Liu and Y. Zhang, Tuning the selectivity of N-alkylated styrylquinolinium dyes for sensing of G-quadruplex DNA, *Bioorg. Med. Chem.*, 2019, **27**, 552–559.

12 (*a*) Q. Li, Y. Kim, J. Namm, A. Kulkarni, G. R. Rosania, Y. H. Ahn and Y. T. Chang, RNA-selective, live cell imaging probes for studying nuclear structure and function, *Chem. Biol.*, 2006, **13**, 615–623; (*b*) M. Q. Wang, S. Liu, C. P. Tang, A. Raza, S. Li, L. X. Gao, J. Sun and S. P. Guo, Flexible amine-functionalized triphenylamine derivative as a fluorescent "light-up" probe for G-quadruplex DNA, *Dyes Pigm.*, 2017, **136**, 78–84; (*c*) A. Manna and S. Chakravorti, Modification of a Styryl Dye Binding Mode with Calf Thymus DNA in Vesicular Medium: From Minor Groove to Intercalative, *J. Phys. Chem. B*, 2012, **116**, 5226–5233; (*d*) Z.-Q. Liu, S.-T. Zhuo, J.-H. Tan, T.-M. Ou, D. Li, L.-Q. Gu and Z.-S. Huang, Facile syntheses of disubstituted bis(vinylquinolinium)benzene derivatives as G-quadruplex DNA binders, *Tetrahedron*, 2013, **69**, 4922–4932; (*e*) Y.-J. Lu, D.-P. Hu, K. Zhang, W.-L. Wong and C.-F. Chow, New pyridinium-based fluorescent dyes: A comparison of symmetry and side-group effects on G-Quadruplex DNA binding selectivity and application in live cell imaging, *Biosens. Bioelectron.*, 2016, **81**, 373–381.

13 A. Granzhan and H. Ihmels, Playing Around with the Size and Shape of Quinolizinium-Derivatives: Versatile Ligands for Duplex, Triplex, Quadruplex and Abasic Site-Containing DNA, *Synlett*, 2016, **27**, 1775–1793.

14 A. Granzhan, H. Ihmels and M. Tian, The benzo[*b*]quinolizinium ion as a water-soluble platform for the fluorimetric detection of biologically relevant analytes, *ARKIVOC*, 2015, **vi**, 494.

15 (*a*) L. Chang, C. Liu, S. He, Y. Lu, S. Zhang, L. Zhao and X. Zeng, Novel styryldehydropyridocolinium derivative as turn-on fluorescent probe for DNA detection, *Sens.*

Actuators, B, 2014, **202**, 483–488; (*b*) H. Yao, L. Chang, C. Liu, X. Jiao, S. He, H. Liu and X. Zeng, A Novel Styryldehydropyridocolinium Homodimer: Synthesis and Fluorescence Properties Upon Interaction with DNA, *J. Fluoresc.*, 2015, **25**, 1637–1643; (*c*) E. Zacharioudakis, T. Cañeque, R. Custodio, S. Müller, A. M. Cuadro, J. J. Vaquero and R. Rodriguez, Quinolizinium as a new fluorescent lysosomotropic probe, *Bioorg. Med. Chem. Lett.*, 2017, **27**, 203–207; (*d*) M. A. Martín, B. del Castillo, J. Ezquerra and J. Alvarez-Builla, Quinolizinium Salts as Fluorescent Probes for N-Nucleophiles, *Anal. Chim. Acta*, 1985, **170**, 89–94; (*e*) P. Martin, M. A. Martin, B. del Castillo and I. Cayre, Polarity effect on fluorescence of styryl derivatives of quinolizinium salts in micellar media, *Anal. Chim. Acta*, 1988, **205**, 129–137.

16 (*a*) Z. J. Ning and H. Tian, Triarylamine: a promising core unit for efficient photovoltaic materials, *Chem. Commun.*, 2009, **37**, 5483–5495; (*b*) R. Chennoufi, H. Bougherara, N. Gagey-Eilstein, B. Dumat, E. Henry, F. Subra, S. Bury-Moné, F. Mahuteau-Betzer, P. Tauc, M. P. Teulade-Fichou and E. Deprez, Mitochondria-targeted Triphenylamine Derivatives Activatable by Two-Photon Excitation for Triggering and Imaging Cell Apoptosis, *Sci. Rep.*, 2016, **6**, 21458; (*c*) M. Q. Wang, W.-X. Zhu, Z.-Z. Song, S. Li and Y.-Z. Zhang, A triphenylamine-based colorimetric and fluorescent probe with donor–bridge–acceptor structure for detection of G-quadruplex DNA, *Bioorg. Med. Chem. Lett.*, 2015, **25**, 5672–5676.

17 (*a*) R. S. Juang, H. W. Wen, M. T. Chen and P. C. Yang, Enhanced sensing ability of fluorescent chemosensors with triphenylamine-functionalized conjugated polyfluorene, *Sens. Actuators, B*, 2016, **231**, 399–411; (*b*) S. Koersten and G. J. Mohr, Star-Shaped Tripodal Chemosensors for the Detection of Aliphatic Amines, *Chem. – Eur. J.*, 2011, **17**, 969–975; (*c*) T. Liu, F. Huo, C. Yin, J. Li, J. Chao and Y. Zhang, A triphenylamine as a fluorophore and maleimide as a bonding group selective turn-on fluorescent imaging probe for thiols, *Dyes Pigm.*, 2016, **128**, 209–214; (*d*) M. Q. Wang, L. X. Gao, Y. F. Yang, X. N. Xiong, Z. Y. Zheng, S. Li, Y. Wu and L. L. Ma, A triphenylamine derivative as a naked-eye and light-up fluorescent probe for G-quadruplex DNA, *Tetrahedron Lett.*, 2016, **57**, 5042–5046; (*e*) I. Pont, J. González-García, M. Inclán, M. Reynolds, E. Delgado-Pinar, M. T. Albelda, R. Vilar and E. García-España, Aza-Macrocyclic Triphenylamine Ligands for G-Quadruplex Recognition, *Chem. – Eur. J.*, 2018, **24**, 10850–10858.

18 L. F. Tietze and U. Beifuss, in *Comprehensive Organic Synthesis*, ed. B. M. Trost, Pergamon, Oxford, 1991.

19 (*a*) A. Richards and T. S. Stevens, Synthesis and properties of dehydropyridocolinium salts, *J. Chem. Soc.*, 1958, 3067–3073; (*b*) O. F. Beumel Jr., W. N. Smith and B. Rybalka, Preparation of 2- and 4-Picolyllithium, *Synthesis*, 1974, 43–45.

20 G. Marcelo, S. Pinto, T. Cañeque, I. F. A. Mariz, A. M. Cuadro, J. J. Vaquero, J. M. G. Martinho and E. M. S. Maçôas, Nonlinear Emission of Quinolizinium-Based Dyes with Application in Fluorescence Lifetime Imaging, *J. Phys. Chem. A*, 2015, **119**, 2351–2362.

21 F. Arbeloa, P. R. Ojeda and I. Arbeloa, Flourescence self-quenching of the molecular forms of Rhodamine B in aqueous and ethanolic solutions, *J. Lumin.*, 1989, **44**, 105–112.

22 M. A. Martin, M. Ballesteros and B. D. Castillo, The influence of solvent polarity and viscosity on fluorescence of quinolizinium salts, *Anal. Chim. Acta*, 1985, **170**, 95–100.

23 (*a*) M. Shortreed, R. Kopelman, M. Kuhn and B. Hoyland, Fluorescent Fiber-Optic Calcium Sensor for Physiological Measurements, *Anal. Chem.*, 1996, **68**, 1414–1418; (*b*) W. Lin, L. Yuan, Z. Cao, Y. Feng and L. Long, A Sensitive and Selective Fluorescent Thiol Probe in Water Based on the Conjugate 1,4-Addition of Thiols to α, β-Unsaturated Ketones, *Chem. – Eur. J.*, 2009, **15**, 5096–5103.

24 F. H. Stootman, D. M. Fisher, A. Rodger and J. R. Aldrich-Wright, *Analyst*, 2006, **131**, 1145.

25 E. M. Rezler, J. Seenisamy, S. Bashyam, M. Y. Kim, E. White, D. Wilson and L. H. Hurley, Telomestatin and Diseleno Sapphyrin Bind Selectively to Two Different Forms of the Human Telomeric G-Quadruplex Structure, *J. Am. Chem. Soc.*, 2005, **127**, 9439–9447.

26 (*a*) O. van den Berg, W. F. Jager and S. J. Picken, 7-Dialkylamino-1-alkylquinolinium Salts: Highly Versatile and Stable Fluorescent Probes, *J. Org. Chem.*, 2006, **71**, 2666–2676; (*b*) A. Granzhan, H. Ihmels and G. Viola, 9-Donor-Substituted Acridizinium Salts: Versatile Environment-Sensitive Fluorophores for the Detection of Biomacromolecules, *J. Am. Chem. Soc.*, 2007, **129**, 1254–1267.

27 B. Heyne, Self-assembly of organic dyes in supramolecular aggregates, *Photochem. Photobiol. Sci.*, 2016, **15**, 1103–1114.

28 (*a*) M. A. Haidekker and E. A. Theodorakis, Molecular rotors—fluorescent biosensors for viscosity and flow, *Org. Biomol. Chem.*, 2007, **5**, 1669–1678; (*b*) A. K. Chibisov, G. V. Zakharova and H. Görner, Effects of substituents in the polymethine chain on the photoprocesses in indodicarbocyanine dyes, *J. Chem. Soc., Faraday Trans.*, 1996, **92**, 4917–4925; (*c*) M. S. A. Abdel-Mottaleb, R. O. Loutfy and R. Lapouyade, Non-radiative deactivation channels of molecular rotors, *J. Photochem. Photobiol., A*, 1989, **48**, 87–93.

29 Y. Hong, J. W. Y. Lam and B. Z. Tang, Aggregation-induced emission, *Chem. Soc. Rev.*, 2011, **40**, 5361–5388.

30 W. Sbliwa, G. Matusiak and B. Bachowska, An Overview of the Optical and Electrochemical Methods for Detection of DNA – Drug Interactions, *Croat. Chem. Acta*, 2006, **79**, 513.

31 (*a*) B. Norden, A. Rodger and T. Dafforn, *Linear Dichroism and Circular Dichroism*, RSC Publishing, Cambridge, 2010; (*b*) T. Šmidlehner, I. Piantanida and G. Pescitelli, Polarization spectroscopy methods in the determination of interactions of small molecules with nucleic acids – tutorial, *Beilstein J. Org. Chem.*, 2018, **14**, 84–105.

32 B. Norden and T. Kurucsev, Analysing DNA complexes by circular and linear dichroism, *J. Mol. Recognit.*, 1994, **7**, 141–156.

33 (*a*) N. Narayanaswamy, S. Das, P. K. Samanta, K. Banu, G. P. Sharma, N. Mondal, S. K. Dhar, S. K. Pati and T. Govindaraju, Sequence-specific recognition of DNA minor groove by an NIR-fluorescence switch-on probe and its potential applications, *Nucleic Acids Res.*, 2015, **43**, 8651–8663; (*b*) X. B. Fu, D. D. Liu, Y. Lin, W. Hu, Z. W. Mao and X. Y. Le, Water-soluble DNA minor groove binders as potential chemotherapeutic agents: synthesis, characterization, DNA binding and cleavage, antioxidation, cytotoxicity and HSA interactions, *Dalton Trans.*, 2014, **43**, 8721–8737.

34 S. Murphy, S. A. Bright, F. E. Poynton, T. McCabe, J. A. Kitchen, E. B. Veale, D. C. Williams and T. Gunnlaugsson, Synthesis, photophysical and cytotoxicity evaluations of DNA targeting agents based on 3-amino-1,8-naphthalimide derived Tröger's bases, *Org. Biomol. Chem.*, 2014, **12**, 6610–6623.

35 (*a*) H. Ihmels and L. Thomas, in *Materials Science of DNA Chemistry*, ed. J. I. Jin, CRC Press, Boca Raton, 2011, p. 49; (*b*) Y. Xie, V. K. Tam and Y. Tor, in *The chemical biology of nucleic acids*, ed. G. Mayer, John Wiley & Sons, Chichester, 2010, p. 115; (*c*) I. Haq, in *Nucleic acids in chemistry and biology*, ed. G. M. Blackburn, M. J. Gait, D. Loakes and D. M. Williams, Royal Society of Chemistry, Cambridge, 2006, p. 341.

36 (*a*) S. Neidle, DNA minor-groove recognition by small molecules, *Nat. Prod. Rep.*, 2001, **18**, 291–309; (*b*) Y. Liu, A. Kumar, S. Depauw, R. Nhili, M. H. David-Cordonnier, M. P. Lee, M. A. Ismail, A. A. Farahat, M. Say, S. Chackal-Catoen, A. Batista-Parra, S. Neidle, D. W. Boykin and W. D. Wilson, Water-Mediated Binding of Agents that Target the DNA Minor Groove, *J. Am. Chem. Soc.*, 2011, **133**, 10171–10183.

37 (*a*) A. Tawani, S. K. Mishra and A. Kumar, Structural insight for the recognition of G-quadruplex structure at human c-myc promoter sequence by flavonoid Quercetin, *Sci. Rep.*, 2017, **7**, 3600; (*b*) N. Ranjan, K. F. Andreasen, S. Kumar, D. H. Volpe and D. P. Arya, Aminoglycoside binding to Oxytricha nova telomeric DNA, *Biochemistry*, 2010, **49**, 9891–9903.

38 (*a*) I. Manet, F. Manoli, B. Zambelli, G. Andreano, A. Masi, L. Cellai and S. Monti, Affinity of the anthracycline antitumor drugs Doxorubicin and Sabarubicin for human telomeric G-quadruplex structures, *Phys. Chem. Chem. Phys.*, 2011, **13**, 540–551; (*b*) W.-B. Wu, S.-H. Chen, J.-Q. Hou, J.-H. Tan, T.-M. Ou, S.-L. Huang, D. Li, L.-Q. Gu and Z.-S. Huang, Disubstituted 2-phenyl-benzopyranopyrimidine derivatives as a new type of highly selective ligands for telomeric G-quadruplex DNA, *Org. Biomol. Chem.*, 2011, **9**, 2975–2986; (*c*) Y. J. Lu, T. M. Ou, J. H. Tan, J. Q. Hou, W. Y. Shao, D. Peng, N. Sun, X. D. Wang, W. B. Wu, X. Z. Bu, Z. S. Huang, D. L. Ma, K. Y. Wong and L. Q. Gu, 5-N-Methylated Quindoline Derivatives as Telomeric G-Quadruplex Stabilizing Ligands: Effects of 5-N Positive Charge on Quadruplex Binding Affinity and Cell Proliferation, *J. Med. Chem.*, 2008, **51**, 6381–6392.

39 (*a*) H. Sun, Y. Tang, J. Xiang, G. Xu, Y. Zhang, H. Zhang and L. Xu, Spectroscopic studies of the interaction between quercetin and G-quadruplex DNA, *Bioorg. Med. Chem. Lett.*, 2006, **16**, 3586–3589; (*b*) T. Yamashita, T. Uno and Y. Ishikawa, Stabilization of guanine quadruplex DNA by the binding of porphyrins with cationic side arms, *Bioorg. Med. Chem.*, 2005, **13**, 2423–2430.

40 A. K. Jain and S. Bhattacharya, Interaction of G-Quadruplexes with Nonintercalating Duplex-DNA Minor Groove Binding Ligands, *Bioconjugate Chem.*, 2011, **22**, 2355–2368.

41 R. N. Dsouza, U. Pischel and W. M. Nau, Fluorescent Dyes and Their Supramolecular Host/Guest Complexes with Macrocycles in Aqueous Solution, *Chem. Rev.*, 2011, **111**, 7941–7980.

42 (*a*) K. Faulhaber, A. Granzhan, H. Ihmels, D. Otto, L. Thomas and S. Wells, Studies of the fluorescence light-up effect of amino-substituted benzo[*b*]quinolizinium derivatives in the presence of biomacromolecules, *Photochem. Photobiol. Sci.*, 2011, **10**, 1535–1545; (*b*) R. Bortolozzi, H. Ihmels, L. Thomas, M. Tian and G. Viola, 9-(4 Dimethylaminophenyl) benzo[*b*]quinolizinium: A Near-Infrared Fluorophore for the Multicolor Analysis of Proteins and Nucleic Acids in Living Cells, *Chem. – Eur. J.*, 2013, **19**, 8736–8741.

43 (*a*) T. Cañeque, A. M. Cuadro, J. Alvarez-Builla, J. Pérez-Moreno, K. Clays, O. Castaño, J. L. Andrés and J. J. Vaquero, Novel charged NLO chromophores based on quinolizinium acceptor units, *Dyes Pigm.*, 2014, **101**, 116–121; (*b*) B. Dumat, G. Bordeau, E. Faurel-Paul, F. Mahuteau-Betzer, N. Saettel, G. Metge, C. Fiorini-Debuisschert, F. Charra and M. P. Teulade-Fichou, DNA Switches on the Two-Photon Efficiency of an Ultrabright Triphenylamine Fluorescent Probe Specific of AT Regions, *J. Am. Chem. Soc.*, 2013, **135**, 12697–12706; (*c*) G. Saielli, G. Scorrano, A. Bagno and A. Wakisaka, Solvation of Tetraalkylammonium Chlorides in Acetonitrile–Water Mixtures: Mass Spectrometry and Molecular Dynamics Simulations, *ChemPhysChem*, 2005, **6**, 1307–1315; (*d*) J. Li, K. Guo, J. Shen, W. Yang and M. Yin, A Difunctional Squarylium Indocyanine Dye Distinguishes Dead Cells through Diverse Staining of the Cell Nuclei/Membranes, *Small*, 2014, **10**, 1351–1360.